Inorganic Chemistry

pubs.acs.org/IC

Communication

Creative Construction of a Series of Chiral 3D Indium−Organic Frameworks with a umy Topology

Xin He,[†] Xin Wang,[†] Tianyu Xiao, Shunlin Zhang, and Dunru Zhu*

Cite This: https://dx.doi.org/10.1021/acs.inorgchem.0c02913

Read Online

ACCESS | Metrics & More | Article Recommendations | Supporting Information

ABSTRACT: Using 2,2′-R_2-biphenyl-4,4′-dicarboxylic acid to bind with a *cis*-[$InO_4(\mu_2\text{-}OH)_2$] octahedron, three novel chiral 3D indium−organic frameworks, [$In(\mu_2\text{-}OH)L$] [**1**, L^1, R = $N(CH_3)_2$; **2**, L^2, R = OCH_3; **3**, L^3, R = CH_3], have been hydrothermally synthesized without chiral reagents. Crystal structure analyses reveal that **1**−**3** show an unprecedented 4-connected **umy** topology with the Schläfli symbol ($4^2{\cdot}6^4$). **1** exhibits high water stability and good sorption selectivity of CO_2 over N_2, while **3** displays high C_2H_2, C_2H_4, and C_2H_6 uptake capacity at 273 K.

Metal−organic frameworks (MOFs) involving divalent transition metals have attracted intense attention because of their aesthetic and topological interest and potential applications in gas separation, catalysis, sensors, and proton conductivity and photoluminescence properties.[1−11] However, relatively fewer studies have been reported for the synthesis of MOFs incorporating trivalent main-group metals, especially for indium. One of the main reasons may be the lower abundance of indium in nature. Recently, investigation of indium−organic frameworks (InOFs) has become an active topic of research because of the very low acute toxicities, high chemical stabilities, and intriguing topologies and properties of InOFs.[12,13] Generally, InOFs are built from three typical secondary building units (SBUs), including tetrahedral [$In(CO_2)_4$] monomers, [$In_3O(CO_2)_6$] trimers, and [$In(OH)(CO_2)_2$] chains.[14−16] Among them, 1D straight chains consisting of *trans*-[$InO_4(\mu_2\text{-}OH)_2$] octahedra are commonly found, while 1D helical chains with *cis*-[$InO_4(\mu_2\text{-}OH)_2$] octahedra are quite unusual.[17−19] It is noteworthy that the helical chain can often act as a chiral origin to induce spontaneous resolution upon crystallization of the racemic compounds, resulting in chiral MOFs.[20] This idea is also important for the construction of chiral MOFs from both academic and practical points of view. Nevertheless, chiral MOFs originating from the helix [$In(OH)(CO_2)_2$] chains are rarely reported.[18] Thus, a large number of chiral nets have not been experimentally identified, although they theoretically exist. For example, the topological number of the 4-connected chiral nets is 71 in theory, but only 11 nets have been discovered in practice.[21] Therefore, the exploration of chiral MOFs with a novel topology still remains a big challenge.

Over the past decade, our group has been interested in building MOFs with substituted biphenyl-4,4′-dicarboxylic acid (BPDC).[22−28] Especially, 2,2′-bisubstituted BPDC with an atropisomeric conformation is a potential chiral source because the free rotation of biphenyl about the C−C bond is often restricted if large groups are attached on the phenyl ring, and the resulting MOFs may show an acentric or chiral structure.[29−31] For instance, 2,2′-dimethoxybiphenyl-4,4′-dicarboxylic acid has been used to construct acentric cadmium-based MOFs, which feature an unprecedented 3D/3D heterointerpenetrating framework consisting of a **dia** net and a **bcu** network.[24,25] However, the chiral main-group-based MOFs built directly from 2,2′-bisubstituted BPDC ligands have not been reported until now. On the basis of these considerations, we designed and synthesized a new substituted BPDC ligand, 2,2′-bis(dimethylamino)biphenyl-4,4′-dicarboxylic acid (H_2L^1 in Scheme S1), and expected that the ligand with two large dimethylamino groups could be used to construct chiral MOFs. Herein, when indium was chosen as the metal center, three chiral InOFs, [$In(\mu_2\text{-}OH)L$] (**1**, L^1; **2**, L^2; **3**, L^3), were built successfully from H_2L^1 and two known 2,2′-bisubstituted BPDC ligands, H_2L^2 and H_2L^3 (Scheme S2), under solvothermal conditions. Crystal structure analyses reveal that InOFs **1**−**3** show an unprecedented 4-connected umy topology induced by an 1D helical chain with a rare *cis*-[$InO_4(\mu_2\text{-}OH)_2$] octahedron. Their gas adsorption properties, spectral features, and stabilities have been systematically investigated.

A solvothermal reaction of equimolar $In(NO_3)_3$ and H_2L^{1-3} in a mixture solvent of *N*,*N*-dimethylformamide (DMF)/acetone/water (H_2O) or dimethylacetamide/H_2O produced **1**−**3** in a yield of 70, 58, and 85%, respectively (see the Supporting Information, SI). Structural analyses reveal that isomorphous **1**−**3** crystallize in the hexagonal $P6_522$ space group for L-**1**−**3** and in $P6_122$ for the enantiomers D-(**1**−**3** (Table S1). Because **1**−**3** are isostructural, only the structure of L-**1** is discussed in detail. The asymmetric unit of L-**1** consists of 0.5 In^{3+} ion, 0.5 $(L^1)^{2-}$ ligand, and 0.5 $\mu_2\text{-}OH^-$ ion (Figure S1). Each In^{3+} center is coordinated by two *cis*-

Received: September 30, 2020

oriented μ_2-OH^- ions (O3 and $O3^i$) and four carboxyl oxygen atoms (O1, $O1^{ii}$, $O2^i$, and $O2^{iii}$) from four different L^1 ligands to form a distorted [InO_6] octahedron where O1, $O1^{ii}$, O3, and $O3^i$ are in the equatorial plane, while $O2^i$ and $O2^{iii}$ sit in the axial positions (Figures 1 and S2). The In1−O1 and In1−

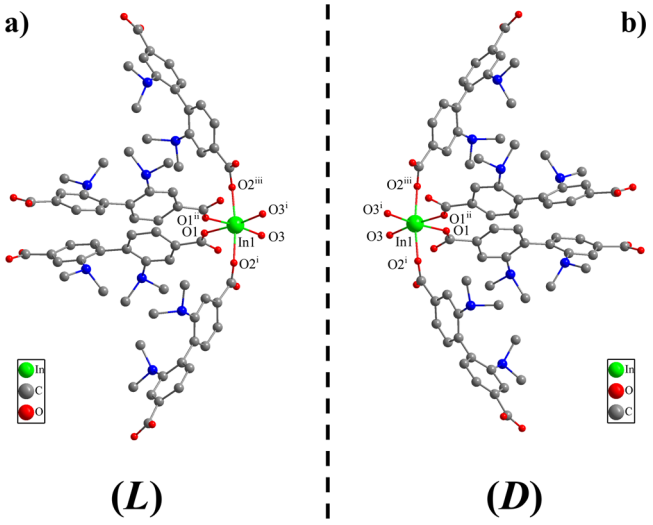

Figure 1. *cis*-[$InO_4(\mu_2$-$OH)_2$] octahedron in L-**1** (a) and D-**1** (b).

$O2^i$ distances are 2.150(2) and 2.154(3) Å, respectively. Each μ_2-OH^- bridge links two In^{3+} ions with an equidistance of 2.0811(13) Å and a In1−O3−$In1^{iv}$ angle of 119.1(1)° (Table S2). All In−O bond lengths are comparable to the related InOFs.[17−19] Each adjacent In^{3+} ion is bridged by a μ_2-OH^- ion and two carboxylic groups to produce a 1D helical [In(μ_2-OH)$(COO)_2$] chain with an In1···$In1^i$ (i, $1 + x - y$, $1 + x$, $z - {}^1/_6$) distance of 3.5878(2) Å (Figure 2a). Along the *c* axis, there is a pitch of 17.7236(9) Å, which is exactly equal to the *c* dimension of the unit cell. Each 1D helical chain as a chiral source is further connected to six peripheral ones through the biphenyl groups to form a 3D homochiral framework (Figure 2b). This arrangement generates 1D trigonal channels with an edge of 9 Å along the *c* axis (Figure S3). The channels are occupied by one H_2O and two DMF molecules, accounting for the 48.4% solvent-accessible voids of the L-**1** framework.[32] Notably, the chirality of L-**1** may come from the axially chiral conformation of the H_2L^1 ligand owing to the existence of two large dimethylamino groups on the 2 and 2′ positions of the biphenyl ring. This hypothesis can be confirmed by the observation of a big dihedral angle [59.07(2)°] between the biphenyl ring (Table S3) and the solid-state circular dichroism spectra (Figure S4). The present InOFs **1**−**3** are good examples of chirality transfer from an achiral ligand to the 1D helical chain and finally to the homochiral lattices. This result may originate from two elements of chirality: (1) the 2,2′-bisubstituted BPDC ligand is locked into an atropisomeric conformation, and (2) the rare *cis*-coordinated μ_2-OH^- ions can induce 1D [In(μ_2-OH)$(COO)_2]_n$ chains to form a helix, thus promoting the transfer of chirality and a spontaneous resolution.[20]

Topologically, if we neglect the μ_2-OH^- ions and connect all carboxylate carbon atoms in the same way as that shown in Figure 2d, it will give a helical ladder with the carbon atoms at the vertices. In this case, each *cis*-[$InO_4(\mu_2$-$OH)_2$] octahedron can be simplified as a 4-connected node, and the framework of L-**1** is finally a 4-connected chiral **umy** net with ($4^2 \cdot 6^4$) topology (Figure 2e).[33−35] To our knowledge, the present 4-connected chiral network with a **umy** topology has not yet been experimentally observed, although it should theoretically exist (Table S5). Furthermore, when the large dimethylamino groups in the H_2L^1 were changed to two smaller ones (methoxy in H_2L^2 and methyl in H_2L^3), while the *cis*-[$InO_4(\mu_2$-$OH)_2$] SBU remained, the same chiral **umy** net can still be obtained, revealing that self-assembly of the *cis*-[$InO_4(\mu_2$-$OH)_2$] SBU with the nonchiral 2,2′-bisubstituted BPDC is an effective strategy for the construction of uninodal chiral 3D MOFs.

The experimental powder X-ray diffraction (PXRD) patterns of **1**−**3** are basically identical with the respective simulated ones, indicating the high phase purity of the bulk products of **1**−**3** (Figures S10−S12). When the crystals of **1** are immersed in H_2O for 1 month, their PXRD peaks are in good agreement with the simulated ones, revealing that **1** is highly water-stable. Moreover, the framework of **1** can also be retained in a pH = 2 aqueous solution for 1 day (Figure S10), which is very unusual in the carboxylate-based 3D InOFs.[18,36−38] In the thermogravimetric analysis (TGA) curve of **1**, the first observed weight loss (26.3%) between 298 and 548 K is due to the loss of one H_2O and two DMF molecules (calcd 26.4%; Figure S13). The framework of **1** collapses above 673 K, and the final residue is In_2O_3 at 813 K (the observed loss of 22.1% and calcd 22.3%). The TGA results of **2** and **3** are similar to those of **1** (Figures S14 and S15), further supporting the isostructural nature of **1**−**3**.

The 55.9% solvent-accessible volume of **2** is smaller than 58.7% of **3** because the size of methoxy in H_2L^2 is larger than that of methyl in H_2L^3. To confirm the permanent porosities of **1**−**3**, the N_2 adsorption isotherm at 77 K is determined, and the results show that all InOFs exhibit a reversible type I isotherm, a characteristic of microporous materials (Figures S16−S18). The Brunauer−Emmett−Teller (BET)/Langmuir surface areas of **1**−**3** are 1167/1196, 1460/1524, and 1694/1829 m^2/g, respectively, and the corresponding porosities are 0.46, 0.56, and 0.65 cm^3/g, respectively (Table 1). Because **3** possesses the biggest BET area and porosity among **1**−**3**, the gas adsorption properties of **3** are studied in detail. The CO_2, CH_4, C_2H_2, C_2H_4, and C_2H_6 adsorption isotherms were measured at 273 and 298 K, respectively (Figure 3). The saturated CO_2, CH_4, C_2H_2, C_2H_4, and C_2H_6 adsorption of **3** at 273 K are 87.5, 32.2, 134.4, 122.5, and 125 cm^3/g, respectively (Table S4), while the N_2 adsorption is only 7.1 cm^3/g. At 298 K, the CO_2, CH_4, C_2H_2, C_2H_4, and C_2H_6 uptake capacities of **3** decrease to 48.9, 21.0, 85.6, 80.2, and 92.5 cm^3/g, respectively, while the N_2 adsorption is merely 2.9 cm^3/g. Thus, **3** shows high C1/C2 gas uptakes compared to the InOFs with similar BET surface area and porosity (Table S4). The CO_2 adsorption value of **3** at 273 K is larger than that (64 cm^3/g) found in a related InOF (FJI-C1) with a similar BET area (1726 m^2/g) but quite smaller than those (190.8 and 129 cm^3/g) in two related InOFs (CPM-200-In/Mg and JLU-Liu18) with the same porosity.[39−41] However, the C_2H_2 and C_2H_6 adsorption values of **3** at 273 K are almost equal to the corresponding ones (135.9 and 123.6 cm^3/g) found in FJI-C1, while the C_2H_4 adsorption value of **3** is larger than that (85.2 cm^3/g) in FJI-C1. Notably, **2** shows the highest CO_2 adsorption capacity of 111.2 cm^3/g at 273 K, which is comparable to the known InOF (JLU-Liu7, 113 cm^3/g) with a smaller BET area (879 m^2/g).[38] The better affinity of **2** with

https://dx.doi.org/10.1021/acs.inorgchem.0c02913
Inorg. Chem. XXXX, XXX, XXX−XXX

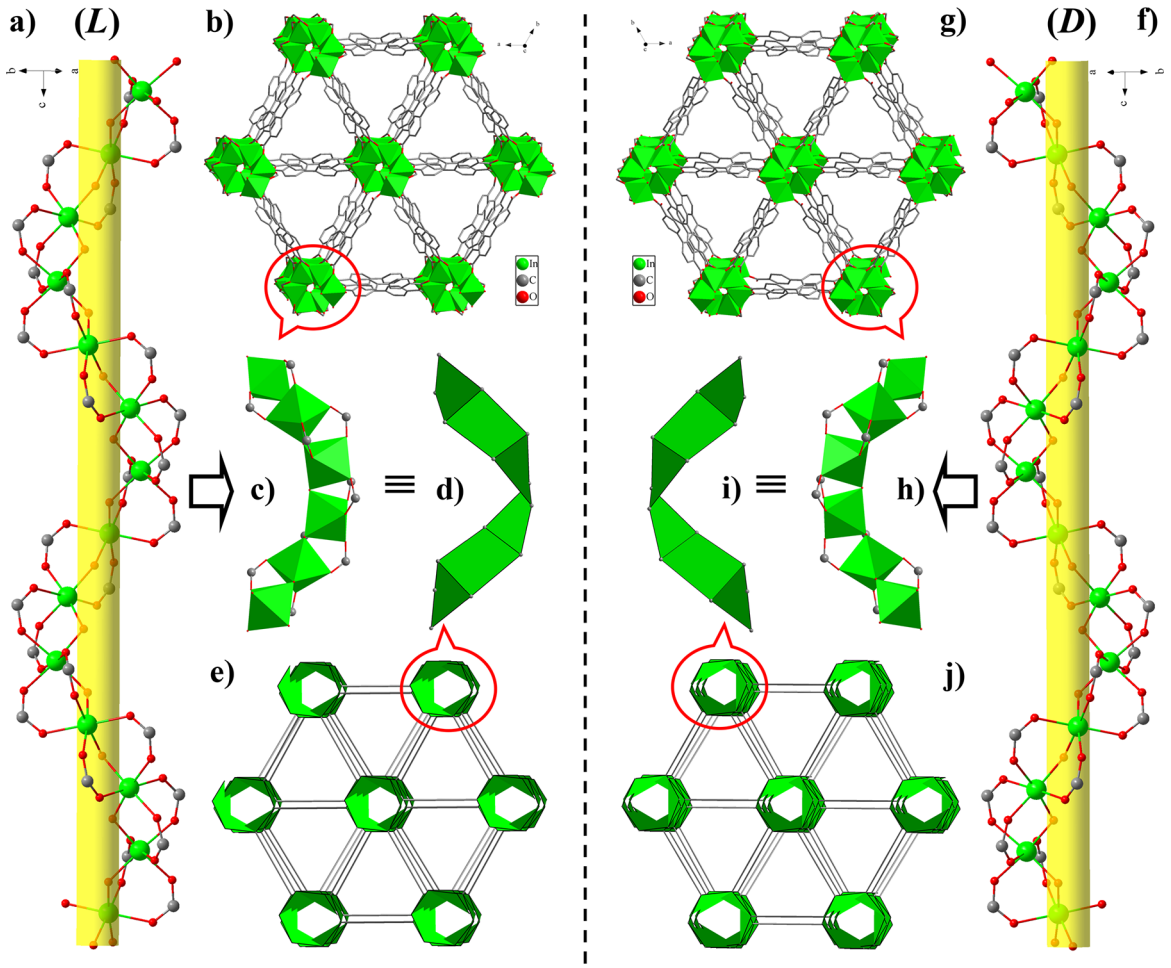

Figure 2. Structure of **1**, with all dimethylamino groups and hydrogen atoms omitted for clarity. 1D helical $[In(\mu_2\text{-}OH)(COO)_2]$ chain in L-(**1**) (a) and D-(**1**) (f). One 1D chain shown as polyhedra linked to six neighboring ones by the biphenyl groups to form a 3D chiral framework in L-(**1**) (b) and D-(**1**) (g). Parts of the 1D helical chain shown as polyhedra in L-(**1**) (c) and D-(**1**) (h). Helical ladder formed in L-(**1**) (d) and D-(**1**) (i) if all of the carboxylate carbon atoms are connected. 4-connected 3D chiral network with a novel **umy** topology in L-(**1**) (e) and D-(**1**) (j).

Table 1. Pore Volume, Surface Area, Gas Uptake Capacity, CO_2 Adsorption Heat (Q_{st}), and Selectivity of CO_2/N_2 (50:50) and CO_2/CH_4 (50:50) for InOFs 1−3 at 273 K

		surface area, m^2/g		gas uptake,[c] cm^3/g STP							selectivity[e]	
InOF	V_p, cm^3/g	BET[a]	Langmuir[b]	CO_2	N_2	CH_4	C_2H_2	C_2H_4	C_2H_6	CO_2 Q_{st},[d] kJ/mol	CO_2/N_2	CO_2/CH_4
1	0.46	1167	1196	91.2	5.5	23.3		95.3		21.8	27.6	4.9
2	0.56	1460	1524	111.2	6.3					24.2	25.9	
3	0.65	1694	1829	87.5	7.1	32.2	134.4	122.5	125	21.4	23.0	2.3

[a]Calculated by the BET method. [b]Calculated by the Langmuir method. [c]At 760 mmHg. [d]Calculated by the virial method. [e]Calculated by Henry's law at 273 K.

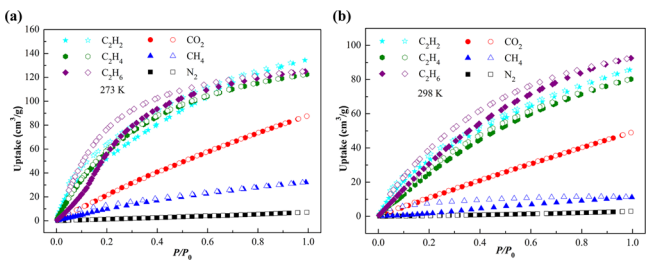

Figure 3. Gas sorption isotherms for **3** at (a) 273 and (b) 298 K. Solid symbols: adsorption. Open symbols: desorption.

CO_2 is attributed to the bigger adsorption enthalpy Q_{st} (24.2 kJ/mol), which is simulated by the virial method (Table 1). On the basis of Henry's law, we calculated the CO_2/N_2 separation selectivity, which is evaluated from the single-component isotherm data. The selective separation ratios of CO_2/N_2 for **1**−**3** are 27.6, 25.9, and 23.0, respectively. Notably, the good separation ratio of CO_2/N_2 and high water stability make **1** a promising candidate for industrial postcombustion gas separation applications.

In summary, by selecting different 2,2′-bisubstituted BPDC to assemble with a 4-connected *cis*-$[InO_4(\mu_2\text{-}OH)_2]$ SBU, we successfully constructed three chiral 3D MOFs with an unprecedented 4-connected **umy** topology. This creative strategy may offer a general method for designing and

https://dx.doi.org/10.1021/acs.inorgchem.0c02913
Inorg. Chem. XXXX, XXX, XXX−XXX

synthesizing novel chiral MOF materials that may have potential applications in asymmetric catalysis. Exploration of the present InOFs as catalysts is in progress.

■ ASSOCIATED CONTENT

Supporting Information

The Supporting Information is available free of charge at https://pubs.acs.org/doi/10.1021/acs.inorgchem.0c02913.

Synthetic details and experimental data (PDF)

Accession Codes

CCDC 2023607−2023612 contain the supplementary crystallographic data for this paper. These data can be obtained free of charge via www.ccdc.cam.ac.uk/data_request/cif, or by emailing data_request@ccdc.cam.ac.uk, or by contacting The Cambridge Crystallographic Data Centre, 12 Union Road, Cambridge CB2 1EZ, UK; fax: +44 1223 336033.

■ AUTHOR INFORMATION

Corresponding Author

Dunru Zhu − *State Key Laboratory of Materials-Oriented Chemical Engineering, College of Chemical Engineering, Nanjing Tech University, Nanjing 211816, P. R. China;* orcid.org/0000-0003-2124-498X; Email: zhudr@njtech.edu.cn

Authors

Xin He − *State Key Laboratory of Materials-Oriented Chemical Engineering, College of Chemical Engineering, Nanjing Tech University, Nanjing 211816, P. R. China*

Xin Wang − *State Key Laboratory of Materials-Oriented Chemical Engineering, College of Chemical Engineering, Nanjing Tech University, Nanjing 211816, P. R. China; School of Chemical and Environmental Engineering, Jiangsu University of Technology, Changzhou 213001, P. R. China*

Tianyu Xiao − *State Key Laboratory of Materials-Oriented Chemical Engineering, College of Chemical Engineering, Nanjing Tech University, Nanjing 211816, P. R. China*

Shunlin Zhang − *State Key Laboratory of Materials-Oriented Chemical Engineering, College of Chemical Engineering, Nanjing Tech University, Nanjing 211816, P. R. China*

Complete contact information is available at: https://pubs.acs.org/10.1021/acs.inorgchem.0c02913

Author Contributions

†These authors contributed equally.

Notes

The authors declare no competing financial interest.

■ ACKNOWLEDGMENTS

This work was financially supported by the National Natural Science Foundation of China (Grant 21476115) and Natural Science Foundation of Jiangsu Province (Grant BK20181374). X.W. thanks the Natural Science Foundation of the Department of Education of Jiangsu Province (Grant 18KJB150013) for financial support. S.Z. acknowledges support from Postgraduate Research & Practice Innovation Program of Jiangsu Province (KYCX20_1027).

■ REFERENCES

(1) Li, J.-R.; Sculley, J.; Zhou, H.-C. Metal-organic frameworks for separations. *Chem. Rev.* **2012**, *112*, 869−932.

(2) Duan, J. G.; Jin, W. Q.; Krishna, R. Natural gas purification using a porous coordination polymer with water and chemical stability. *Inorg. Chem.* **2015**, *54*, 4279−4284.

(3) Nenoff, T. M. MOF membranes put to the test. *Nat. Chem.* **2015**, *7*, 377−378.

(4) Qin, T.; Gong, J.; Ma, J.; Wang, X.; Wang, Y.; Xu, Y.; Shen, X.; Zhu, D. R. A 3D MOF showing unprecedented solvent-induced single-crystal-to-single-crystal transformation and excellent CO_2 adsorption selectivity at room temperature. *Chem. Commun.* **2014**, *50*, 15886−15889.

(5) Cui, Y.; Yue, Y.; Qian, G.; Chen, B. Luminescent functional metal-organic frameworks. *Chem. Rev.* **2012**, *112*, 1126−1162.

(6) Toyao, T.; Miyahara, K.; Fujiwaki, M.; Kim, T.; Dohshi, S.; Horiuchi, Y.; Matsuoka, M. Immobilization of Cu complex into Zr-based MOF with bipyridine units for heterogeneous selective oxidation. *J. Phys. Chem. C* **2015**, *119*, 8131−8137.

(7) Zheng, J.; Wu, M.; Jiang, F.; Su, W.; Hong, M. Stable porphyrin Zr and Hf metal-organic frameworks featuring 2.5 nm cages: high surface areas, SCSC transformations and catalyses. *Chem. Sci.* **2015**, *6*, 3466−3470.

(8) Cho, W.; Lee, H. J.; Choi, G.; Choi, S.; Oh, M. Dual changes in conformation and optical properties of fluorophores within a metal-organic framework during framework construction and associated sensing event. *J. Am. Chem. Soc.* **2014**, *136*, 12201−12204.

(9) Yuan, S.; Zou, L.; Li, H.; Chen, Y.-P.; Qin, J.; Zhang, Q.; Lu, W.; Hall, M. B.; Zhou, H. C. Flexible zirconium metal-organic frameworks as bioinspired switchable catalysts. *Angew. Chem.* **2016**, *128*, 10934−10938.

(10) Pang, J.; Yuan, S.; Qin, J.; Wu, M.; Lollar, C. T.; Li, J.; Huang, N.; Li, B.; Zhang, P.; Zhou, H. C. Enhancing pore-environment complexity using a trapezoidal linker: toward stepwise assembly of multivariate quinary metal-organic frameworks. *J. Am. Chem. Soc.* **2018**, *140*, 12328−12332.

(11) Sun, C. Y.; Wang, X. L.; Qin, C.; Jin, J. L.; Su, Z. M.; Huang, P.; Shao, K. Z. Solvatochromic behavior of chiral mesoporous metal-organic frameworks and their applications for sensing small molecules and separating cationic dyes. *Chem. - Eur. J.* **2013**, *19*, 3639−3645.

(12) Chen, X.; Jiang, H.; Li, X.; Hou, B.; Gong, W.; Wu, X.; Han, X.; Zheng, F.; Liu, Y.; Jiang, J.; Cui, Y. Chiral phosphoric acids in metal-organic frameworks with enhanced acidity and tunable catalytic selectivity. *Angew. Chem., Int. Ed.* **2019**, *58*, 14748−14757.

(13) Yuan, Y.; Li, J.; Sun, X.; Li, G.; Liu, Y.; Verma, G.; Ma, S. Indium-organic frameworks based on dual secondary building units featuring halogen-decorated channels for highly effective CO_2 fixation. *Chem. Mater.* **2019**, *31*, 1084−1091.

(14) Zheng, S.-T.; Zuo, F.; Wu, T.; Irfanoglu, B.; Chou, C.; Nieto, R. A.; Feng, P.; Bu, X. Cooperative assembly of three-ring-based zeolite-type metal-organic frameworks and johnson-type dodecahedra. *Angew. Chem., Int. Ed.* **2011**, *50*, 1849−1852.

(15) Liu, Y.; Eubank, J. F.; Cairns, A. J.; Eckert, J.; Kravtsov, V. C.; Luebke, R.; Eddaoudi, M. Assembly of metal−organic frameworks (MOFs) based on indium-trimer building blocks: a porous MOF with soc topology and high hydrogen storage. *Angew. Chem., Int. Ed.* **2007**, *46*, 3278−3283.

(16) Qian, J.; Jiang, F.; Su, K.; Pan, J.; Liang, L.; Mao, F.; Hong, M. Constructing crystalline heterometallic indium-organic frameworks by the bifunctional method. *Cryst. Growth Des.* **2015**, *15*, 1440−1445.

(17) Mazaj, M.; Volkringer, C.; Loiseau, T.; Kaučič, V.; Férey, G. Synthesis and crystal structure of a new MOF-type indium pyromellitate (MIL-117) with infinite chains of unusual *cis* connection of octahedra $InO_4(OH)_2$. *Solid State Sci.* **2011**, *13*, 1488−1493.

(18) Qian, J. J.; Jiang, F. L.; Yuan, D. Q.; Wu, M. Y.; Zhang, S. Q.; Zhang, L. J.; Hong, M. C. Highly selective carbon dioxide adsorption in a water-stable indium-organic framework material. *Chem. Commun.* **2012**, *48*, 9696−9698.

(19) Vougo-Zanda, M.; Wang, X.; Jacobson, A. J. Influence of ligand geometry on the formation of In-O chains in metal-oxide organic frameworks (MOOFs). *Inorg. Chem.* **2007**, *46*, 8819−8824.

https://dx.doi.org/10.1021/acs.inorgchem.0c02913
Inorg. Chem. XXXX, XXX, XXX−XXX

(20) Qin, T.; Feng, Z.; Yang, J.; Shen, X.; Zhu, D. Unprecedented three-dimensional hydrogen-bonded *hex* topological chiral lanthanide-organic frameworks built from an achiral ligand. *Acta Crystallogr., Sect. C: Struct. Chem.* **2018**, *74*, 1403−1412.
(21) See the website of the O'Keeffe group at Arizona State University: http://rcsr.anu.edu.au.
(22) Wang, X. Z.; Zhu, D. R.; Xu, Y.; Yang, J.; Shen, X.; Zhou, J.; Fei, N.; Ke, X. K.; Peng, L. M. Three novel metal-organic frameworks with different topologies based on 3,3′-dimethoxy-4,4′-biphenyldicarboxylic acid: syntheses, structures, and properties. *Cryst. Growth Des.* **2010**, *10*, 887−894.
(23) Zhang, H. J.; Wang, X. Z.; Zhu, D. R.; Song, Y.; Xu, Y.; Xu, H.; Shen, X.; Gao, T.; Huang, M. X. Novel 3D lanthanide-organic frameworks with an unusual infinite nanosized ribbon $[Ln_3(\mu_3\text{-}OH)_2(\text{-}CO_2)_6]^+_n$ (Ln = Eu, Gd, Dy): syntheses, structures, luminescence and magnetic properties. *CrystEngComm* **2011**, *13*, 2586−2592.
(24) Xu, H.; Bao, W.; Xu, Y.; Liu, X.; Shen, X.; Zhu, D. An unprecedented 3D/3D hetero-interpenetrated MOF built from two different nodes, chemical composition and topology of networks. *CrystEngComm* **2012**, *14*, 5720−5722.
(25) Luo, R.; Xu, H.; Gu, H. X.; Wang, X.; Xu, Y.; Shen, X.; Bao, W.; Zhu, D. R. Four MOFs with 2,2′-dimethoxy-4,4′-biphenyldicarboxylic acid: syntheses, structures, topologies and properties. *CrystEngComm* **2014**, *16*, 784−796.
(26) Liu, X.; Wang, X.; Gao, T.; Xu, Y.; Shen, X.; Zhu, D. Three 3D lanthanide-organic frameworks with *sra* topology: syntheses, structures, luminescence and magnetic properties. *CrystEngComm* **2014**, *16*, 2779−2787.
(27) Wang, X.; Zhao, J.; Zhao, Y.; Xu, H.; Shen, X.; Zhu, D. R.; Jing, S. Three *sra* topological lanthanide-organic frameworks built from 2,2′-dimethoxy-4,4′-biphenyldicarboxylic acid. *Dalton Trans* **2015**, *44*, 9281−9288.
(28) Zhao, J.; Wang, X.; Zhao, J.; Luo, R.; Shen, X.; Zhu, D.; Jing, S. $[Ln_4@Ln_4]$ matryoshka tetrahedron: a novel secondary building unit. *CrystEngComm* **2016**, *18*, 863−867.
(29) Keene, T. D.; Rankine, D.; Evans, J. D.; Southon, P. D.; Kepert, C. J.; Aitken, J. B.; Sumby, C. J.; Doonan, C. J. Solvent-modified dynamic porosity in chiral 3D kagome frameworks. *Dalton Trans* **2013**, *42*, 7871−7879.
(30) Ferguson, A.; Liu, L.; Tapperwijn, S. J.; Perl, D.; Coudert, F.-X.; Van Cleuvenbergen, S.; Verbiest, T.; van der Veen, M. A.; Telfer, S. G. Controlled partial interpenetration in metal-organic frameworks. *Nat. Chem.* **2016**, *8*, 250−257.
(31) Chen, L.-Z.; Pan, Q.-J.; Cao, X.-X.; Wang, F.-M. Crystal structure, magnetism, and dielectric properties based on the axially chiral ligand 2,2′-dinitro-4,4′-biphenyldicarboxylic acid. *CrystEngComm* **2016**, *18*, 1944−1952.
(32) Sheldrick, G. M. Crystal structure refinement with SHELXL. *Acta Crystallogr., Sect. A: Found. Crystallogr.* **2008**, *64*, 112−122.
(33) Blatov, V. A. *IUCr CompComm Newsletter* **2006**, *7*, 4; http://www.topos.ssu.samara.ru.
(34) Blatov, V. A.; O'Keeffe, M.; Proserpio, D. M. Vertex-, face-, point-, Schläfli-, and Delaney-symbols in nets, polyhedra and tilings: recommended terminology. *CrystEngComm* **2010**, *12*, 44−48.
(35) Alexandrov, E. V.; Blatov, V. A.; Kochetkov, A. V.; Proserpio, D. M. Underlying nets in three-periodic coordination polymers: topology, taxonomy and prediction from a computer-aided analysis of the Cambridge Structural Database. *CrystEngComm* **2011**, *13*, 3947−3958.
(36) Guo, Z.-J.; Yu, J.; Zhang, Y.-Z.; Zhang, J.; Chen, Y.; Wu, Y.; Xie, L.-H.; Li, J.-R. Water-stable In(III)-based metal-organic frameworks with rod-shaped secondary building units: single-crystal to single-crystal transformation and selective sorption of C_2H_2 over CO_2 and CH_4. *Inorg. Chem.* **2017**, *56*, 2188−2197.
(37) Fan, W.; Liu, X.; Wang, X.; Li, Y.; Xing, C.; Wang, Y.; Guo, W.; Zhang, L.; Sun, D. A fluorine-functionalized microporous In-MOF with high physicochemical stability for light hydrocarbon storage and separation. *Inorg. Chem. Front.* **2018**, *5*, 2445−2449.
(38) Luo, J.; Wang, J.; Cao, Y.; Yao, S.; Zhang, L.; Huo, Q.; Liu, Y. Assembly of an indium-porphyrin framework JLU-Liu7: a mesoporous metal-organic framework with high gas adsorption and separation of light hydrocarbons. *Inorg. Chem. Front.* **2017**, *4*, 139−143.
(39) Huang, Y.; Lin, Z.; Fu, H.; Wang, F.; Shen, M.; Wang, X.; Cao, R. Porous anionic indium−organic framework with enhanced gas and vapor adsorption and separation ability. *ChemSusChem* **2014**, *7*, 2647−2653.
(40) Zhai, Q. G.; Bu, X.; Mao, C.; Zhao, X.; Feng, P. Systematic and dramatic tuning on gas sorption performance in heterometallic metal-organic frameworks. *J. Am. Chem. Soc.* **2016**, *138*, 2524−2527.
(41) Yao, S.; Wang, D.; Cao, Y.; Li, G.; Huo, Q.; Liu, Y. Two stable 3D porous metal-organic frameworks with high performance for gas adsorption and separation. *J. Mater. Chem. A* **2015**, *3*, 16627−16632.

https://dx.doi.org/10.1021/acs.inorgchem.0c02913
Inorg. Chem. XXXX, XXX, XXX−XXX